**Supporting Information (*SI Appendix*)**

# FOXD3-mediated transactivation of ALKBH5 promotes neuropathic pain via m$^6$A-dependent stabilization of 5-HT3A mRNA in sensory neurons

Zitong Huang [a, e, #], Yuan Zhang [b, d, e, #], Shoupeng Wang [a, e, #], Renfei Qi [a, e], Yu Tao [a, e], Yufang Sun [a, e], Dongsheng Jiang [c], Xinghong Jiang [a, e], Jin Tao [a, d, e, f, *]

[a] Department of Physiology and Neurobiology, Suzhou Medical College of Soochow University, Suzhou 215123, P.R. China;

[b] Clinical Research Center of Neurological Disease & Department of Geriatrics, The Second Affiliated Hospital of Soochow University, Suzhou 215004, P.R. China;

[c] Institute of Regenerative Biology and Medicine, Helmholtz Zentrum München, Munich 81377, Germany;

[d] Jiangsu Key Laboratory of Neuropsychiatric Diseases, Soochow University, Suzhou 215123, P.R. China;

[e] Centre for Ion Channelopathy, Soochow University, Suzhou 215123, P.R. China;

[f] MOE Key Laboratory of Geriatric Diseases and Immunology, Suzhou Medical College of Soochow University, Suzhou 215123, P.R. China.

[#] These authors contribute to this work equally.

**Running title:** ALKBH5 promotes neuropathic pain

***To whom correspondence should be addressed:**

Dr. Jin Tao, Department of Physiology and Neurobiology, Suzhou Medical College of Soochow University, 199 Ren-Ai Road, Suzhou 215123, P.R. China. E-mail: taoj@suda.edu.cn

**This PDF file includes:**

**SI Materials and Methods**

**SI References**

**SI Figures S1 to S36;**

**SI Tables S1 to S2**

## SI Materials and Methods

### Animal model and behavioral tests

All protocols for animal experiments in this study were conducted in accordance with the NIH guidelines for animal research and the International Association for the Study of Pain and were approved by the Animal Care and Use Committee of Soochow University. Adult male Sprague–Dawley rats (8-10 weeks) were housed under a 12 h-12 h light-dark cycle, with food and water *ad libitum*. Every effort was made to reduce the number of animals used in research and minimize their suffering. The animals were allowed to habituate to the housing facilities for at least 1 week before the surgery. An intraoral approach was used to create a chronic constriction injury to the infraorbital nerve (CCI-ION) model of trigeminal neuropathic pain (1-3). In brief, rats were anesthetized with isoflurane, and an incision (~1 cm) was made starting at the first molar along the gingivobuccal margin in rat buccal mucosa. Glass rods were used to dissect the left ION close to the infraorbital foramen. The two 4-0 silk sutures were tied loosely around the infraorbital nerve and spaced 3–4 mm apart. Sham-operated rats were subjected to the same anesthesia and surgical procedure, but the unilateral nerve was manipulated without ligation. All behavioral tests were executed by individuals blinded to the experimental design. Behavioral tests were implemented 2 days before CCI-ION surgery and at designated time points following CCI-ION operation. As demonstrated in our previous reports (1, 4, 5), the escape threshold to orofacial mechanical stimuli was examined using *von* Frey filaments (Ugo Basile). The left vibrissal pad area of the rat was stimulated successively with *von* Frey filaments from 2 g to 15 g. To avoid tissue damage and because the bending force already

rotated the rat's head, a filament weight of 15 g was selected as the cutoff threshold. In every set of trials, each *von* Frey stimulation was employed three times, with a duration of 2-3 seconds. Head withdrawal or escape in rats was regarded as a positive response in accordance with the previous method initially described by Vos *et al.* (6). Heat sensitivity, expressed as head withdrawal latency, was tested by radiant heat using the Hargreaves apparatus (Ugo Basile) as previously described (5, 7). The intensity of the radiant heat was adjusted so yield a basal latency between 8 and 12 seconds, with a cutoff latency of 18 seconds to avoid tissue damage. The orofacial stimulation test was conducted to measure the hypersensitivity to the mechanical stimulation in the trigeminal-mediated area, using the Orofacial Stimulation Test system (Ugo Basile) (5, 8). Following a 12-hour fasting food period, rats underwent 1 week of adaptation training. After a ten-minute familiarization with the environment, the drinking window was opened, and the testing animal was timed for ten minutes to allow drinking the milk. The total contact time that the rat spent acquiring the reward was analyzed using the ORO software (Ugo Basile).

**Intra-TG drug application**

Intra-TG injection was performed following the procedure as described previously (1, 4). Drugs/reagents were delivered slowly in a volume of 3 μl, and a 10-min needle retention period was used before the needle was removed. Ondansetron (Abcam) was diluted to 3 mM in dimethyl sulfoxide (DMSO). 2'-O-Methyl- and 5'-cholesteryl-modified siRNAs for Alkbh5 (ALKBH5-siNRA, Ribo Bio), Hdac11 (HDAC11-siRNA, Ribo Bio), 5-HT3A (5-HT3A–siRNA, GenePharm) and the relevant scrambled control siRNAs (NC-siRNA), tagged with 6-carboxyfluorescein (6-FAM), were dissolved in RNase-free water, and were intra-TG administrated daily for 2 consecutive days. The siRNA sequences are summarized in Table S1. The neuron-specific promoter (*hSyn*) combinatorial lentiviral vectors, including lenti-hSyn-ALKBH5-up, lenti-hSyn-HDAC11-up and negative controls (NC-up), carrying the eGFP gene, were purchased from GenePharma (Shanghai).

**Immunoblot analysis**

Immunoblotting was conducted as previously described (1, 4, 9). In brief, equal amounts of

protein samples (30 μg) were separated by SDS–PAGE and then transferred onto polyvinylidene fluoride membranes (Millipore). After blocking with 5% nonfat milk, the blots were incubated with primary antibodies against the following: ALKBH5 (rabbit, 1:2000, Proteintech), FTO (rabbit, 1:1000, Proteintech), WTAP (rabbit, 1:1000, Proteintech), METTL3 (rabbit, 1:1000, Abcam), METTL14 (rabbit, 1:1000, ABclonal), FOXD3 (mouse, 1:1000, Santa Cruz), G3BP1 (rabbit, 1:2000, Proteintech), YTHDC1 (rabbit, 1:1000, Abcam), YTHDC2 (rabbit, 1:2000, Proteintech), YTHDF1 (rabbit, 1:1000, Proteintech), YTHDF2 (rabbit, 1:2000, Proteintech), YTHDF3 (mouse, 1:500, Santa Cruz), HDAC11(mouse, 1:100, Santa Cruz), H4ac (rabbit, 1:5000, Abcam), H3K27ac (rabbit, 1:5000, Abcam), H3K18ac (rabbit, 1:5000, Abcam), H3K14ac (rabbit, 1:2000, Abcam), H3K9ac (rabbit, 1:1000, Cell Signaling Technology), HAT1 (rabbit, 1:1000, Proteintech), 5-HT3A (rabbit, 1:1000, Abcam), 5-HT3B (rabbit, 1:800, Abcam), H3 (rabbit, 1:600, Abcam) and GAPDH (mouse, 1:10000, Proteintech). Blots were then incubated with appropriate HRP-conjugated secondary antibodies, including goat anti-rabbit IgG (1:8000, R&D Systems) and goat anti-mouse IgG (1:8000, R&D Systems). Blots for acetylation-modified histone antibody were stripped with Western Blot Stripping Buffer (Thermo Fisher Scientific), washed with TBST, blocked again with nonfat milk, and reprobed for total H3, the loading control. The protein bands were detected with Pierce™ ECL Western Blotting Substrate (Thermo Fisher). The ChemiDoc XRS system (Bio-Rad Laboratories) was used to capture the images, and Quantity One software was used to analyze the protein bands.

**Immunofluorescence staining**

Immunostaining was carried out as described previously (1, 4, 10). In brief, fixed TGs were embedded in OCT (Leica) and sectioned with a cryostat (Leica) at a 12-μm thickness. After washing, the tissue sections were treated with PBS containing 0.25% Triton X-100 and 5% goat serum. Subsequently, the sections were incubated with primary antibodies against ALKBH5 (rabbit, 1:500, Proteintech), NF200 (mouse, 1:600, Abcam), $IB_4$ (mouse, 1:400, Sigma), CGRP (mouse, 1:600, Abcam), GS (mouse, 1:500, Abcam), NeuN (mouse, 1:200, Cell Signaling Technology), FOXD3 (mouse, 1:600, Santa Cruz), H3K27ac (mouse, 1:1000, Active Motif), HDAC11 (mouse, 1:100, Santa Cruz), YTHDF2 (rabbit, 1:500, Proteintech), 5-HT3A (mouse,

1:100, Santa Cruz) and 5-HT3A (rabbit, 1:500, Abcam). TG sections were then incubated with the appropriate HRP-conjugated secondary antibody. The slices were mounted with glycerinum or DAPI solution, and then visualized using an upright fluorescence microscope (104C, Nikon). Fluorescent images were recorded using a cooled CCD camera (CoolSNAP HQ2, Photometrics).

**m$^6$A dot blot assay**

Dot blot assays were conducted according to the Bioprotocol database (https://en.bioprotocol.org/e2095). In brief, total RNA was extracted using Takara RNAiso Plus, and mRNA was isolated and purified using PolyATtract® mRNA Isolation Systems (Promega). The mRNA samples were serially diluted to 200/100/50 ng/μl with RNase-free water. Then, the serially diluted mRNA was denatured at 95 °C in a heat block for 3 minutes and immediately placed on ice. Equal volumes of RNA (2 μl) were spotted onto a Hybond $N^+$ membrane (Beyotime). After 15 minutes of UV crosslinking, the membrane was washed, blocked with 5% nonfat milk, and incubated overnight at 4 °C with the anti-m$^6$A antibody (1:2000, Synaptic Systems). Then, dot blots were visualized by the imaging system after incubation with secondary antibody for 1 hour at room temperature. Methylene blue staining was applied to verify that equal amounts of RNA samples were spotted on the membrane.

**Real-time quantitative PCR (RT–qPCR)**

Takara RNAiso Plus was used to extract the total RNA (Takara). The quality and RNA concentrations were determined using a NanoDrop spectrophotometer (Thermo Fisher Scientific). To synthesize cDNA, purified total RNA was reverse-transcribed using the PrimeScript RT Reagent Kit (Takara). qPCR was performed using the ROCHE LightCycler® 96 System with SYBR Green qPCR Master Mix (Takara). The amplification conditions were as follows: 94 °C for 5 min, followed by 40 cycles of 95 °C for 15 s and 60 °C for 60 s. Relative gene expression was normalized to GAPDH expression and analyzed by the comparative $2^{-\Delta\Delta Cq}$ method. The primers used in this study are summarized in Table S2.

**RNA immunoprecipitation (RIP)-PCR**

RIP assays were conducted using a Magna RIP™ RNA-Binding Protein Immunoprecipitation

Kit (Millipore). In brief, TG samples were lysed with RIP lysis buffer comprising RNase and protease inhibitors. Magnetic beads were incubated with 5 μg antibodies against ALKBH5 (Proteintech), G3BP1 (Proteintech), YTHDC1 (Abcam), YTHDC2 (Proteintech), YTHDF1 (Proteintech), YTHDF2 (Proteintech), YTHDF3 (Santa Cruz) or rabbit IgG (Millipore). Next, after 10% of the lysate supernatant was preserved as an RNA input control, the remainder of the samples were then treated with bead-antibody complex with RIP immunoprecipitation buffer containing 0.5 M EDTA and RNAe inhibitor at 4 °C overnight. After washing, the RNA–protein complexes were eluted and decrosslinked by proteinase K digestion buffer. The RNA products were purified and then used for further RT–qPCR analysis as described above.

**Dual-luciferase reporter assay**

The fragments (pGL3-F1, -2129 bp to -9 bp; pGL3-F2, -2129 bp to -393 bp; pGL3-F3, -2129 bp to -874 bp; pGL3-F4, -2129 bp to -1229 bp; pGL3-F5, -2129 bp to -1646 bp) in the *Alkbh5* gene promoter region were amplified by PCR from genomic DNA with the primers (Table S2) to construct the reporter plasmids. The KpnI/NheI cleavage sites of the pGL3-Basic vector (Promega) were used for plasmid construction. The validation of the recombinant plasmid sequences was conducted by DNA sequencing. PC12 cells were cotransfected using Lipofectamine 3000 ™ (Thermo Fisher Scientific) with the different recombinant reporter plasmids (500 ng) and the Renilla reporter vector (pRL-TK, 100 ng). To assess interactions between the transcription factors and the ΔF region of the *Alkbh5* promoter (-874 to -393 bp), 500 ng of overexpression plasmids of MAFB, FOXD3 or SP1 and 100 ng pRL-TK were cotransfected. The indicated MAFB, FOXD3 and SP1 overexpression plasmids were obtained from Sangon Bioengineering Technology (Shanghai). The Dual-Luciferase Reporter Assay System (Promega) was applied to detect the luciferase activities. The reporter activity was determined after normalization of the firefly luciferase enzyme activity to Renilla luciferase activity.

**Chromatin immunoprecipitation (ChIP)-qPCR**

ChIP assays were conducted with the SimpleChIP® Plus Enzymatic Chromatin IP Kit (Cell Signaling Technology) as described previously (1). In brief, tissue samples were cut into pieces,

crosslinked with 1.5% formaldehyde in PBS, and quenched with 2.5 M glycine. Cells were lysed, and nuclei were collected and treated with micrococcal nuclease. After an appropriate amount of sonication, two percent of the supernatant was saved as an input control. The remaining chromatin was then immunoprecipitated with 2 μg of antibodies against FOXD3 (Santa Cruz), H3K27ac (Abcam) or IgG (Millipore) to pull down chromatin. Next, the immunocomplexes were rotationally incubated with ChIP-Grade Protein G Magnetic Beads and then eluted and decrosslinked by proteinase K. The DNA product was purified and collected for further qPCR analyses. The ChIP-specific primers used are shown in Table S2. The enrichment of specific genomic regions was assessed and normalized to the input DNA. PCR products were analyzed on a 2% agarose gel (Sigma).

**Methylated RNA immunoprecipitation (MeRIP)**

The MeRIP assay was performed using the Magna MeRIP™ $m^6A$ Kit (Millipore) according to the manufacturer's guidelines. In brief, total RNA was extracted using TRIzol (Takara) and randomly fragmented into 100 nucleotides or less. RNA samples were then immunoprecipitated with magnetic beads precoated with 10 μg of anti-$m^6A$ antibody (Millipore) or anti-mouse IgG (Millipore). A 10% volume of fragmented RNA was saved as the input control. N6-methyladenosine 5'-monophosphate sodium salt (6.7 mM) was applied to elute $m^6A$-precipitated RNA. The modification of $m^6A$ toward particular genes was determined by MeRIP-qPCR analysis with specific primers (Table S2). The PCR products were analyzed on a 2% agarose gel (Sigma).

**MeRIP sequencing**

MeRIP sequencing and the following data analyses were mainly supported by Shanghai Cloud-Seq Biotech. In brief, total RNA from rat TGs treated with ALKBH5-up and NC-up was extracted and then randomly fragmented into fragments of approximately 200 nt. After ten percent of fragmented mRNA was saved as input, $m^6A$-modified mRNA was immunoprecipitated with anti-$m^6A$ antibodies (Millipore) and eluted. The GenSeq® Low Input Whole RNA Library Prep Kit (GenSeq, Inc.) was used for library preparation of both $m^6A$-enriched mRNAs and input mRNAs. The constructed libraries were quality-controlled using an

Agilent 2100 Bioanalyzer, followed by sequencing on a NovaSeq sequencer (Illumina, Inc.). For MeRIP-seq data analysis, adaptors and low-quality bases of raw reads were trimmed using Cutadapt software (v1.9.3) to obtain clean reads. Sequence reads were aligned to the rat genome version RN5 with HISAT2 software (v2.0.4). MACS software was used to identify methylated genes in each sample. Differentially methylated genes were identified using diffReps software. MeRIP-enriched regions (peaks) were visualized using Integrative Genomics Viewer (IGV).

**RNA stability assay**

PC12 cells were cultured in complete medium containing DMEM/F-12 (Gibco), 10% fetal bovine serum (FBS) and 1% antibiotics. All cells were maintained in a humidified incubator (Thermo Fisher Scientific) at 37 °C and 5% $CO_2$. After digestion with 0.25% trypsin (Sigma), the cells were resuspended in complete medium. Cells were transfected with NC-up or ALKBH5-up using Lipofectamine 3000 (Invitrogen). The cells were treated with 5 μg/ml actinomycin D (J&K Scientific) to terminate transcription. Total RNA was extracted at 0 h, 3 h, 6 h and 9 h after treatment for qPCR analysis.

**Dissociation of TG neurons**

Rat TG neurons were acutely dissociated as previously described (1, 10). In brief, rats were decapitated under anesthesia, and TGs were dissected out rapidly. After removing connective tissue and trimming, the tissues were enzymatically digested with 2.5 mg/ml collagenase D (Roche) at 37 °C for 35 min and then with 1.2 mg/ml trypsin (Sigma) at 37 °C for 20 min. Individual neurons were dissociated by gentle trituration of the ganglia using flame-polished Pasteur pipettes. Then, the cells were plated in a droplet of growth medium on glass coverslips coated with Matrigel (Merck) and maintained in an incubator at 37 °C until recording. Electrophysiological recordings were performed 3–7 h after plating.

**Electrophysiology**

Whole-cell recordings were conducted at room temperature (23 ± 1 °C) in a gap-free pattern as previously described (1, 4, 10). The resistance of the patch pipettes was 3-5 MΩ when filled with pipette solution. 5-HT (10 μM, Sigma) was applied to evoke 5-HT-activated currents. The external solution comprised (in mM) 150 NaCl, 5 KCl, 2.5 $CaCl_2$, 1 $MgCl_2$, 10 HEPES and 10

D-glucose and was adjusted to a pH of 7.4 with NaOH. The internal solution comprised (in mM) 140 KCl, 2 $MgCl_2$, 10 HEPES, 11 EGTA and 5 ATP and was adjusted to a pH of 7.2 with KOH. Current- and voltage-clamp recordings were performed using a Multiclamp 700B amplifier (Molecular Devices). The data were collected using pClamp10 (Axon) and analyzed with Clampfit 10.2 (Molecular Devices). Signals were filtered by an on-board lowpass filter frequency at 2 kHz with a sampling frequency of 10 kHz with a Digidata 1440 A digitizer (Molecular Devices). A well-established etrograde tracer DiI (20 mg/ml, Thermo Fisher) was subcutaneously injected into the cushion of rats. Four days after injection, small-sized TG neurons (soma diameter < 30 μm) were subjected to electrophysiological recording. 5-HT-induced action potential recordings were conducted under current-clamp mode. The external solution comprised (in mM) 128 NaCl, 2 KCl, 2 $CaCl_2$, 2 $MgCl_2$, 25 HEPES, and 30 glucose and was adjusted to a pH of 7.4 with NaOH. The internal solution comprised (in mM) 110 KCl, 25 HEPES, 10 NaCl, 0.3 Na-GTP, 4 Mg-ATP, and 2 EGTA and was adjusted to a pH of 7.4 with KOH. Action potentials were evoked by a 1-s current injection, and the minimal current needed to excite a neuron was the rheobase.

**Data analysis and statistics**

All data are expressed as the mean ± S.E.M. Data acquisition and statistical analysis were performed using Microsoft Excel, ClampFit 10.2 (Molecular Devices), and Prism 8.0 (GraphPad Software). Two groups were compared by a two-tailed, unpaired Student's *t* test. Comparisons among groups were performed by one-way ANOVA. Comparisons among groups with multiple time points were performed by two-way ANOVA. If ANOVA showed significant differences, *post hoc* Bonferroni's test was applied. Differences with $p$ values < 0.05 were considered to be significant.

**SI References:**

1. R. Qi *et al.*, Histone methylation-mediated microRNA-32-5p down-regulation in sensory neurons regulates pain behaviors via targeting Cav3.2 channels. *Proc Natl Acad Sci U S A* **119**, e2117209119 (2022).

2. L. Q. Chen *et al.*, Asymmetric activation of microglia in the hippocampus drives anxiodepressive consequences of trigeminal neuralgia in rodents. *Br J Pharmacol* 10.1111/bph.15994 (2022).
3. E. Gambeta, M. A. Gandini, I. A. Souza, G. W. Zamponi, Ca V 3.2 calcium channels contribute to trigeminal neuralgia. *Pain* **163**, 2315-2325 (2022).
4. H. Wang *et al.*, Brain-derived neurotrophic factor stimulation of T-type Ca(2+) channels in sensory neurons contributes to increased peripheral pain sensitivity. *Sci Signal* **12** (2019).
5. Y. Zhang *et al.*, Neuromedin B receptor stimulation of Cav3.2 T-type Ca(2+) channels in primary sensory neurons mediates peripheral pain hypersensitivity. *Theranostics* **11**, 9342-9357 (2021).
6. B. P. Vos, A. M. Strassman, R. J. Maciewicz, Behavioral evidence of trigeminal neuropathic pain following chronic constriction injury to the rat's infraorbital nerve. *The Journal of neuroscience : the official journal of the Society for Neuroscience* **14**, 2708-2723 (1994).
7. C. M. Kopruszinski, R. C. Reis, E. Bressan, P. W. Reeh, J. G. Chichorro, Vitamin B complex attenuated heat hyperalgesia following infraorbital nerve constriction in rats and reduced capsaicin in vivo and in vitro effects. *European journal of pharmacology* **762**, 326-332 (2015).
8. M. Prochazkova *et al.*, Activation of cyclin-dependent kinase 5 mediates orofacial mechanical hyperalgesia. *Molecular pain* **9**, 66 (2013).
9. Y. Zhang *et al.*, Peripheral pain is enhanced by insulin-like growth factor 1 through a G protein-mediated stimulation of T-type calcium channels. *Sci Signal* **7**, ra94 (2014).
10. J. Cao *et al.*, Electrical stimulation of the superior sagittal sinus suppresses A-type K(+) currents and increases P/Q- and T-type Ca(2+) currents in rat trigeminal ganglion neurons. *J Headache Pain* **20**, 87 (2019).

**SI Figures S1 to S36**

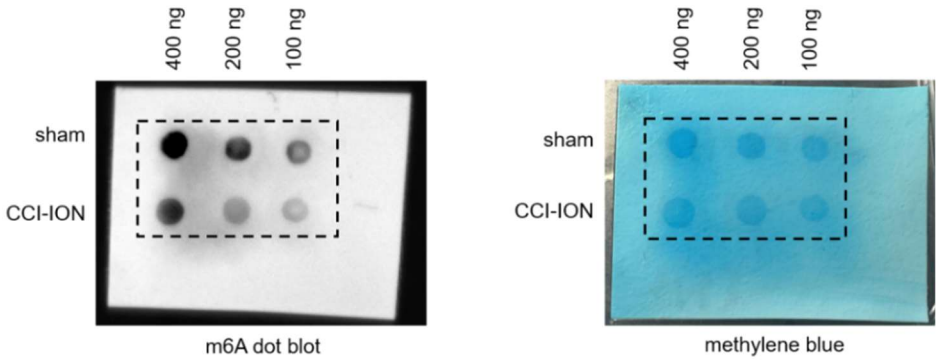


**Fig. S1: m6A levels in rat TGs after CCI-ION or sham-operation.** Shown are the expanded images of dot blots presented in Fig. 1B.

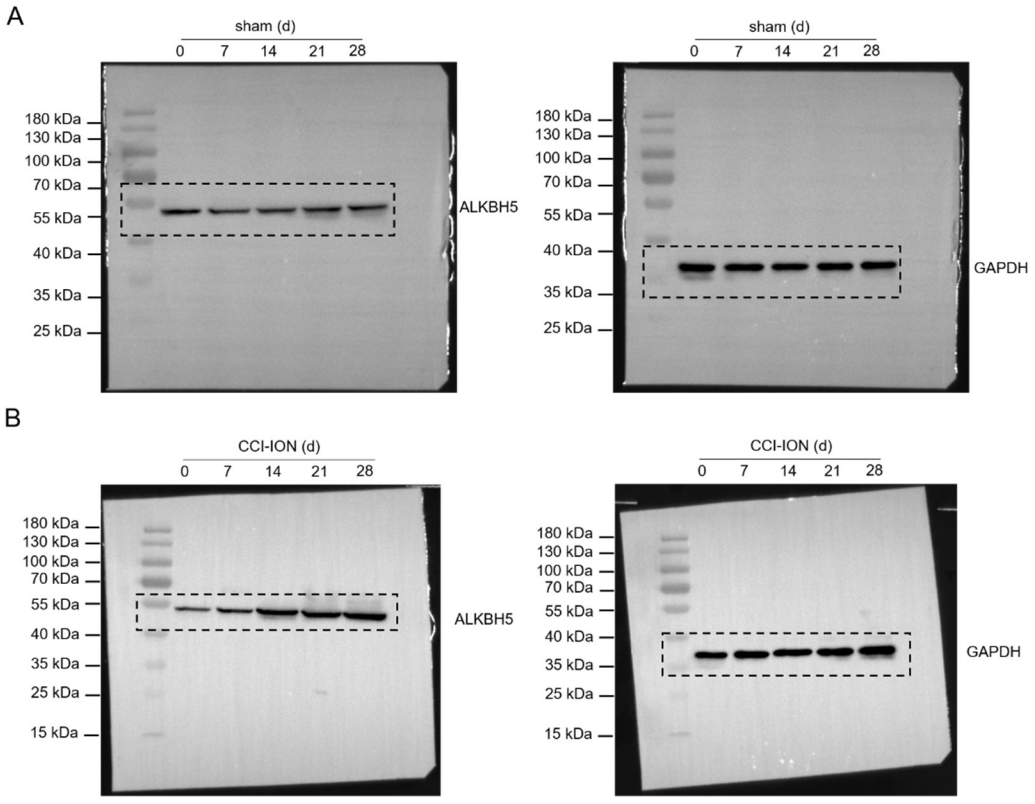


**Fig. S2: Immunoblot analysis of TG ALKBH5 following sham surgery (*A*) or CCI-ION operation (*B*).** Immunoblot images of the selected portion are displayed in Fig. 1E.

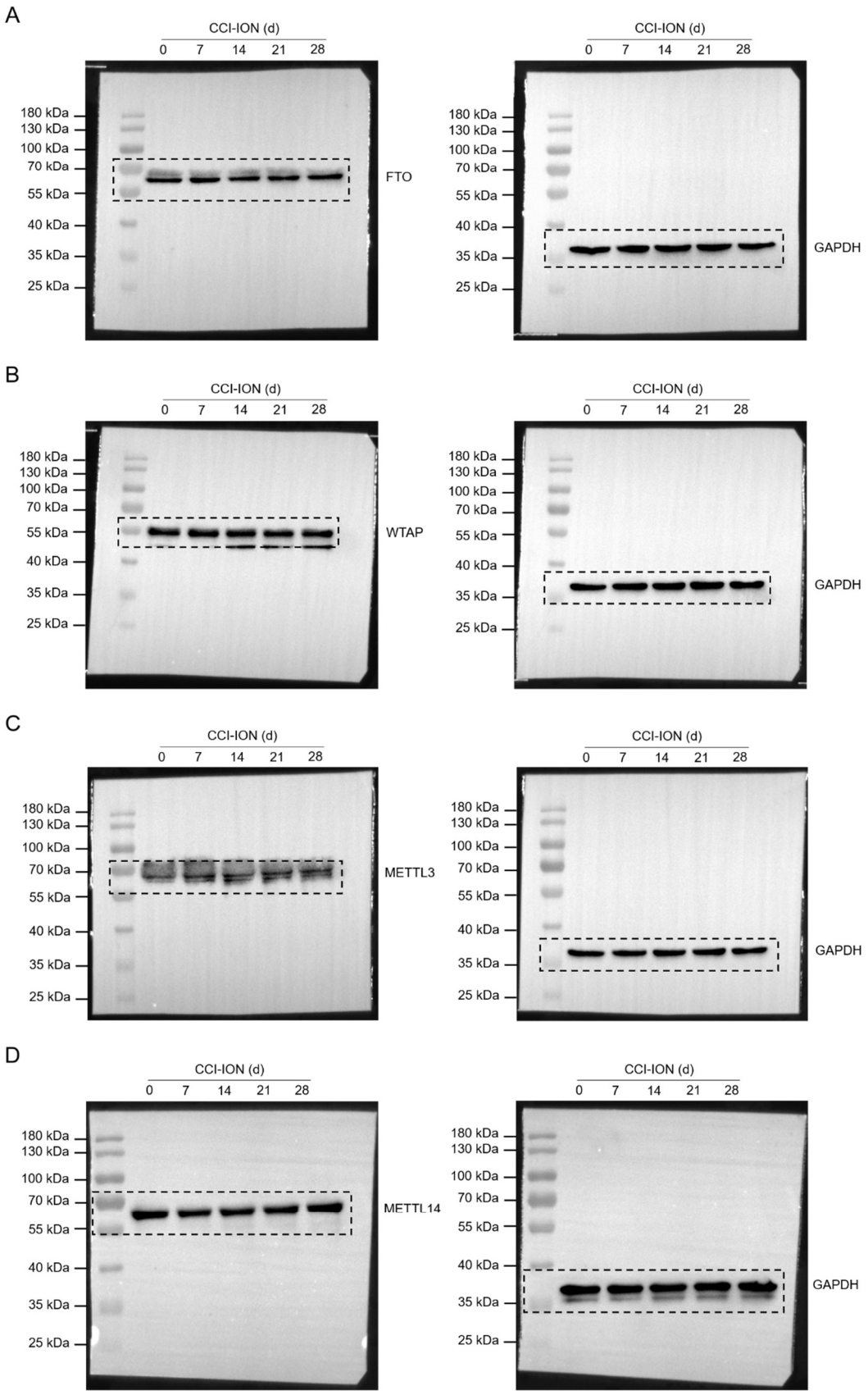


**Fig. S3: Protein expression of FTO (*A*), WTAP (*B*), METTL3 (*C*) and METTL14 (*D*) in rat TGs after CCI-ION.** Western blot images of the selected portion are displayed in Fig. 1F.

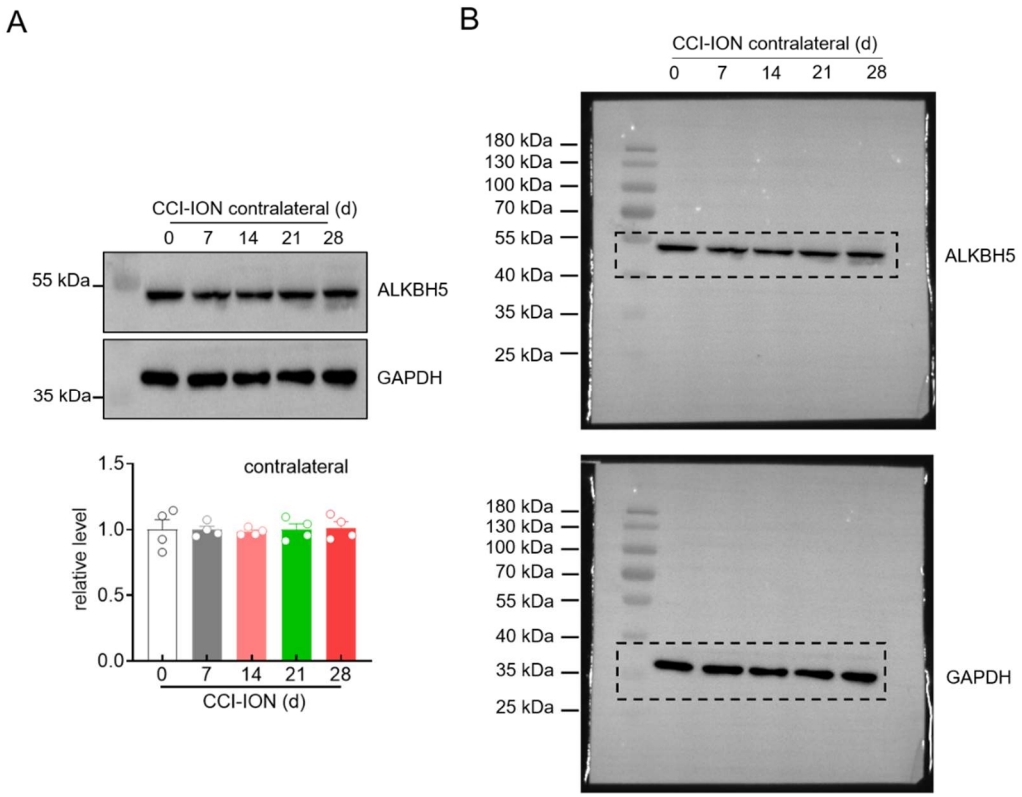


**Fig. S4: Immunoblot analysis of ALKBH5 in the contralateral TG after CCI-ION. (A)** CCI-ION did not affect the protein abundance of ALKBH5 in the contralateral TG following surgery. **(B)** Immunoblot images of the selected portion are displayed in panel *A*.

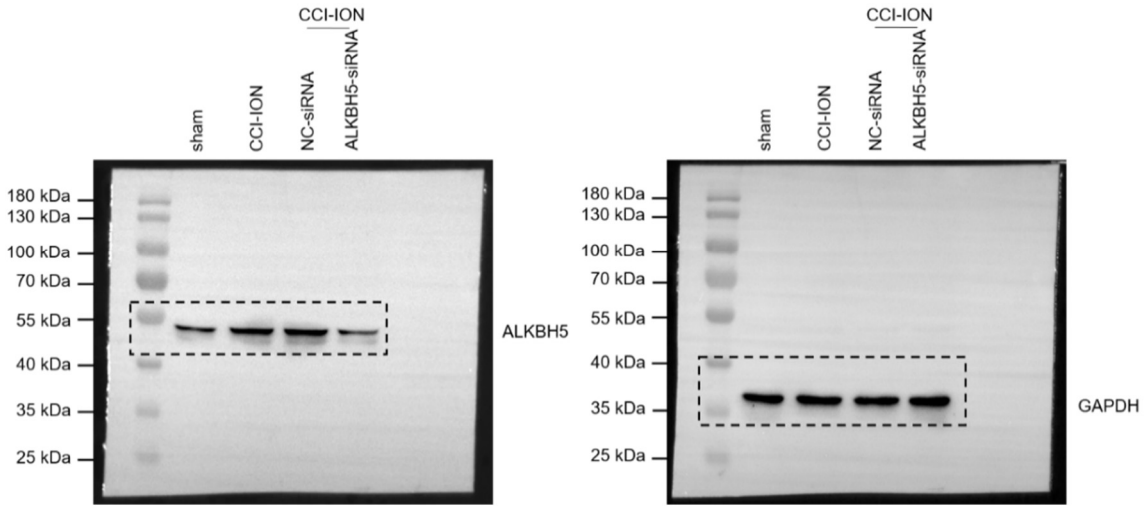


**Fig. S5: Intra-TG administration of ALKBH5-siRNA suppressed the increased ALKBH5 expression in the injured TG 14 days following CCI-ION.** Immunoblot images of the selected portion are displayed in Fig. 2A.

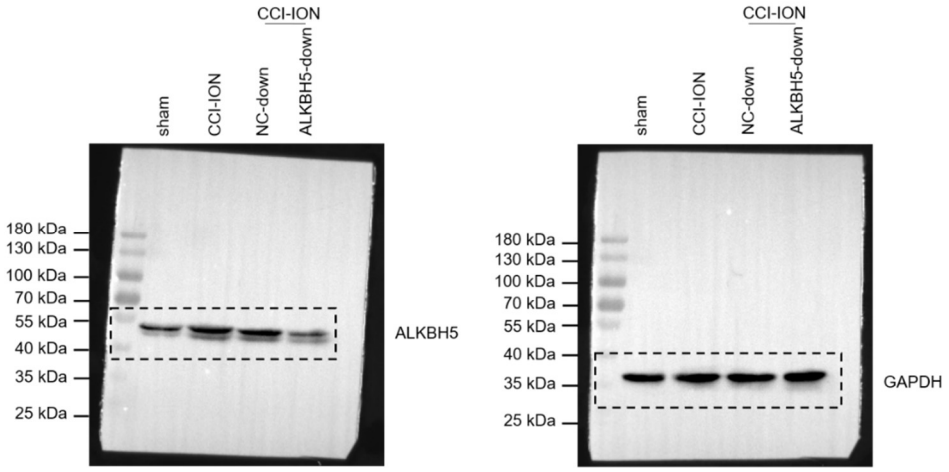


**Fig. S6: Administration of ALKBH5-down suppressed the increased ALKBH5 expression in the injured TG 14 days following CCI-ION.** Immunoblot images of the selected portion are displayed in Fig. 2C.

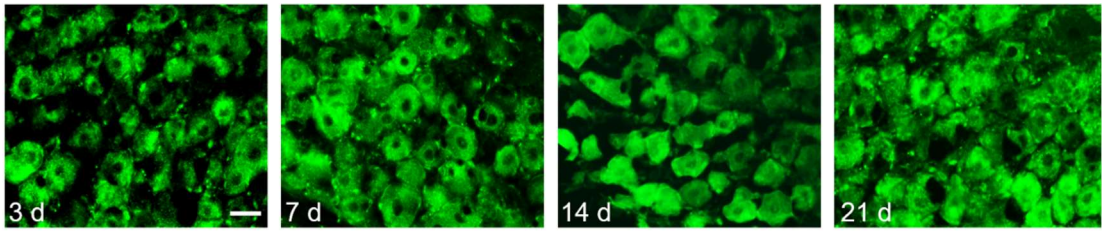


**Fig. S7: Validation of lentiviral delivery in naive TGs.** The eGFP fluorescence was observed in TG neurons at 3 days after intra-TG injection of lenti-hSyn-ALKBH5-up-eGFP (ALKBH5-up) and was maintained on Day 21.

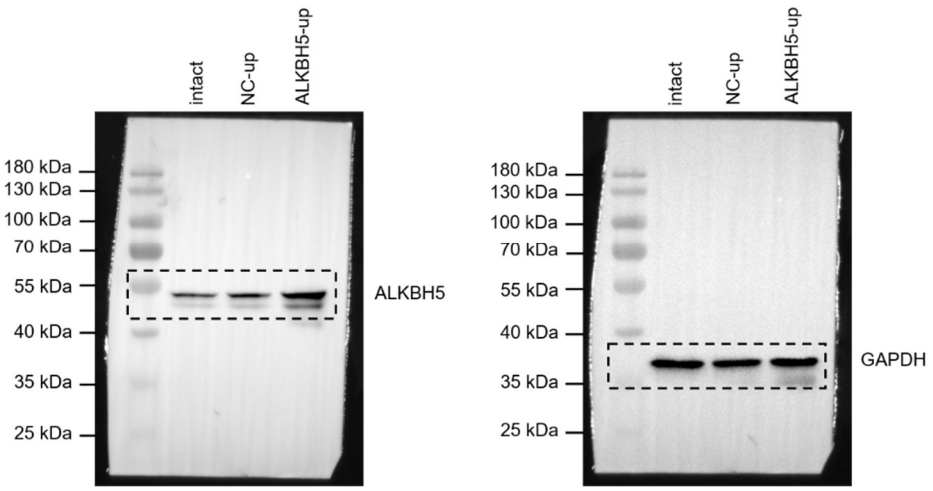


**Fig. S8: Administration of ALKBH5-up increased the protein abundance of ALKBH5 in intact TGs.** Western blot images of the selected portion are displayed in Fig. 2I.

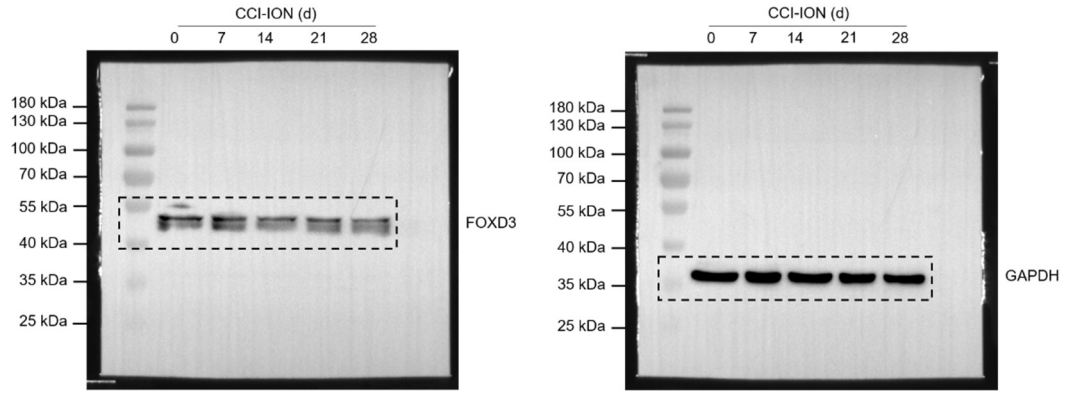


**Fig. S9: Immunoblot analysis of FOXD3 in rat TGs following CCI-ION.** Immunoblot images of the selected portion are displayed in Fig. 3F.

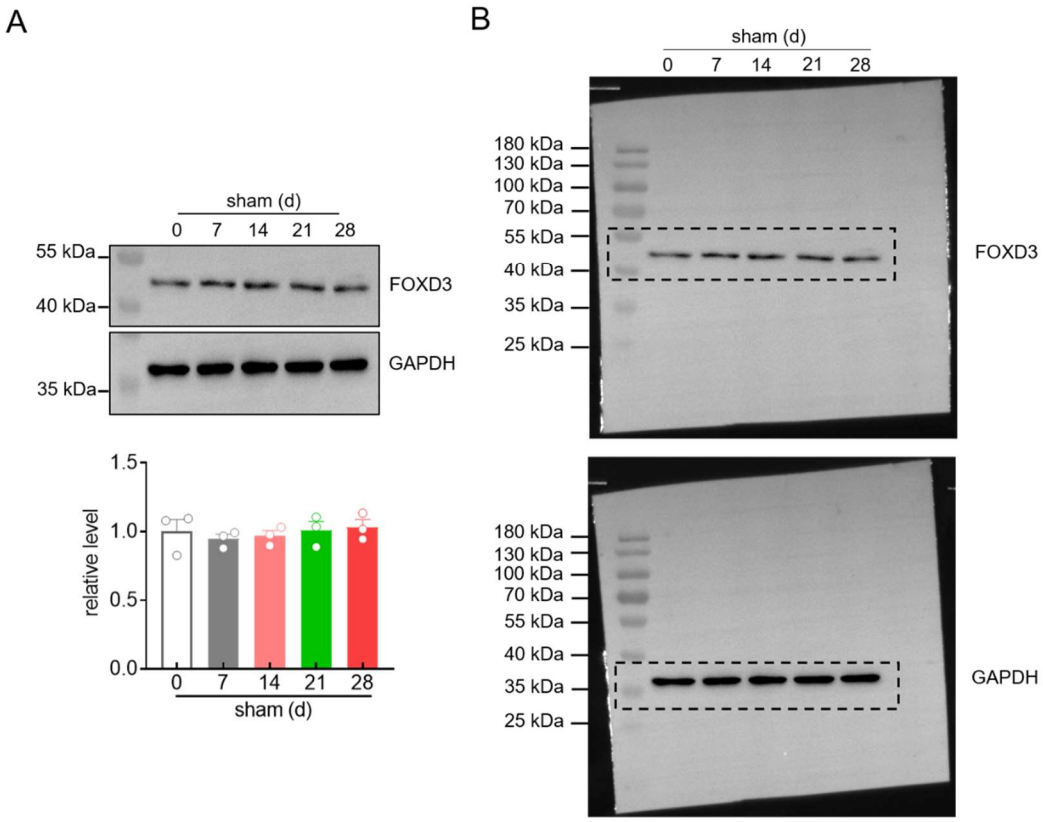


**Fig. S10: Immunoblot analysis of FOXD3 in rat TGs following sham-operation.** (**A**) Sham surgery did not affect the protein abundance of FOXD3 in the ipsilateral TG after sham surgery. (**B**) Western blot images of the selected portion are displayed in panel *A*.

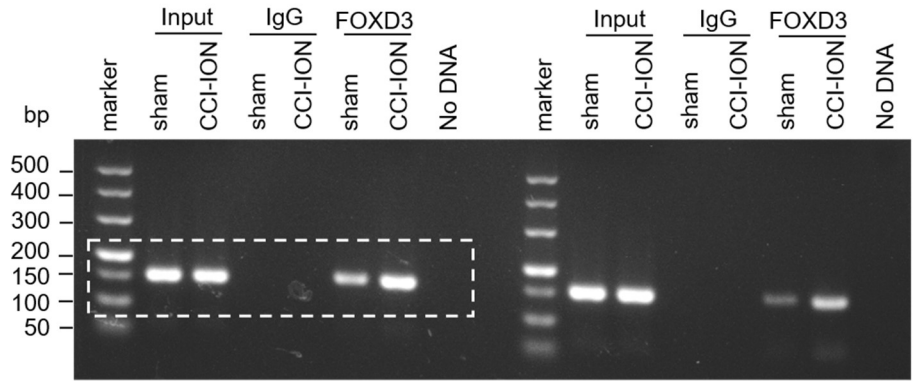


**Fig. S11: ChIP analysis indicating the binding of FOXD3 in the *Alkbh5* promoter in rat TGs after CCI-ION or sham operation.** Shown is the full unedited gel for Fig. 3G.

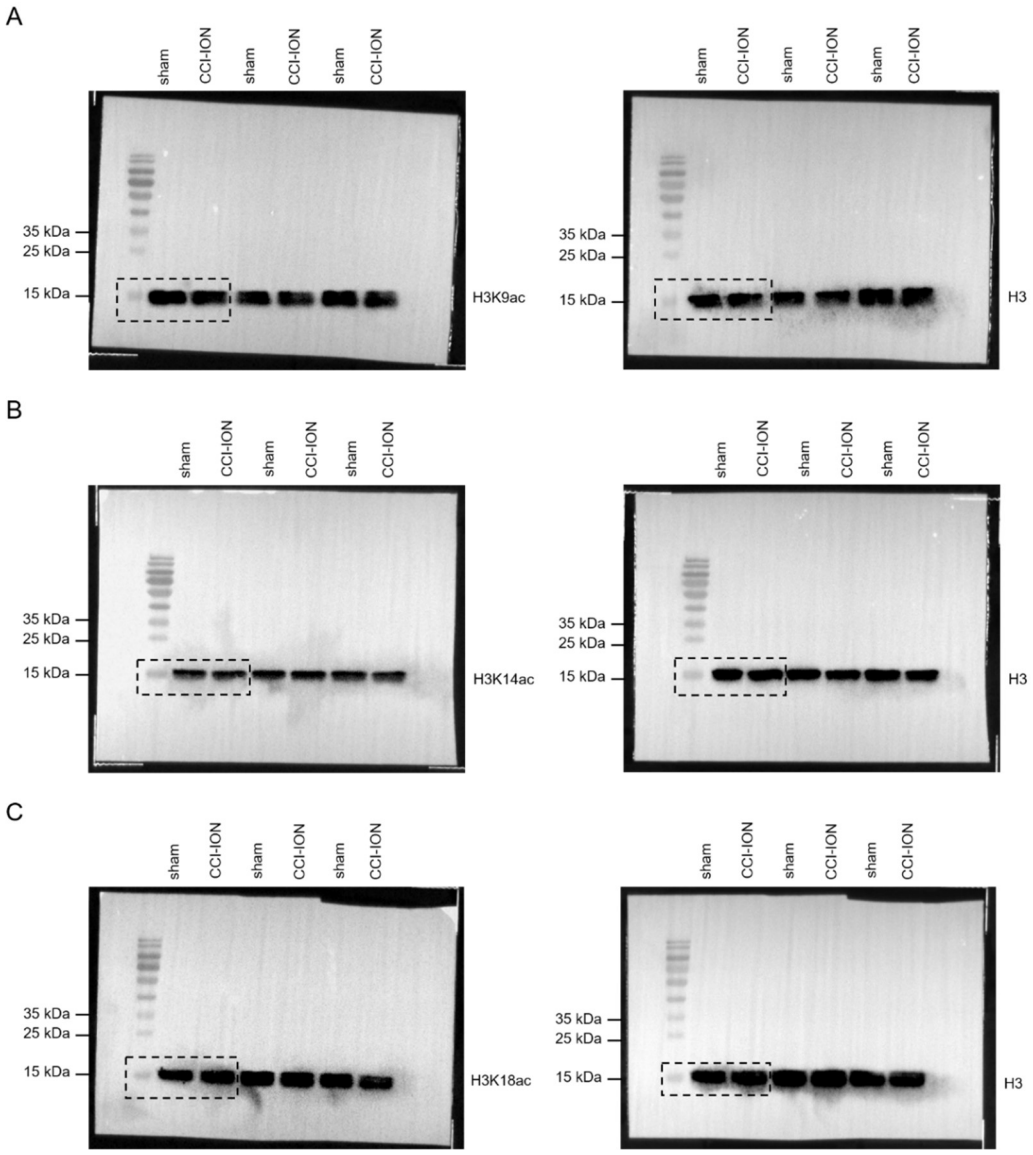

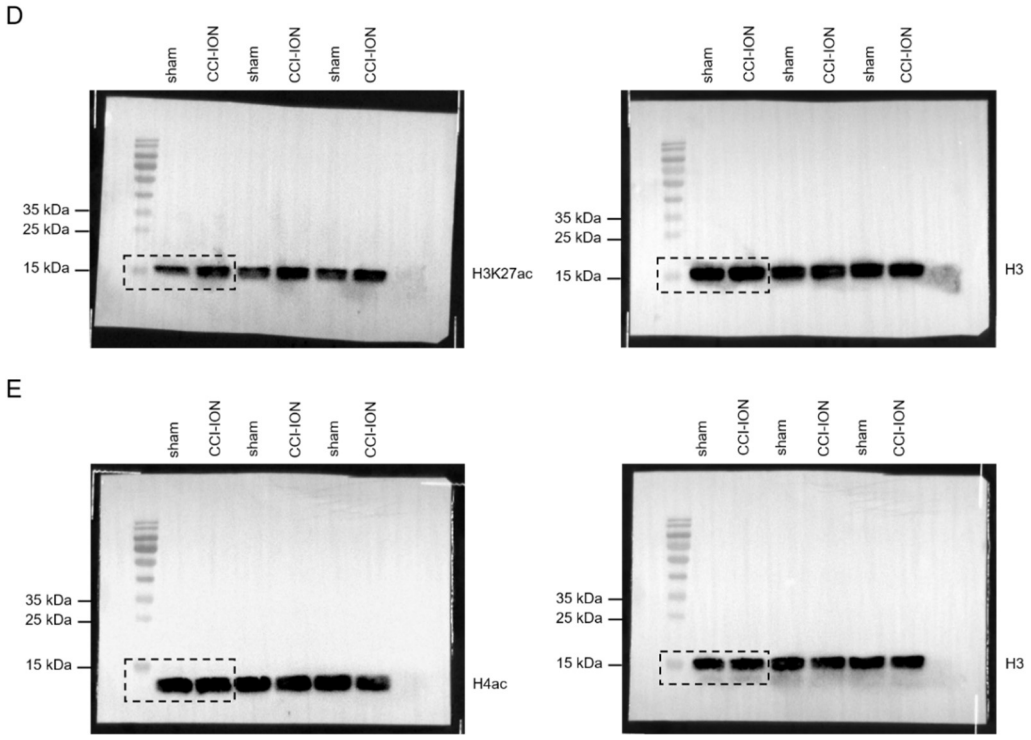


**Fig. S12: Immunoblots showing the protein expression levels of H3K9ac (*A*), H3K14ac (*B*), H3K18ac (*C*), H3K27ac (*D*), and H4ac (*E*) in rat TGs following CCI-ION operation or sham surgery.** Immunoblot images of the selected portion are displayed in Fig. 4A.

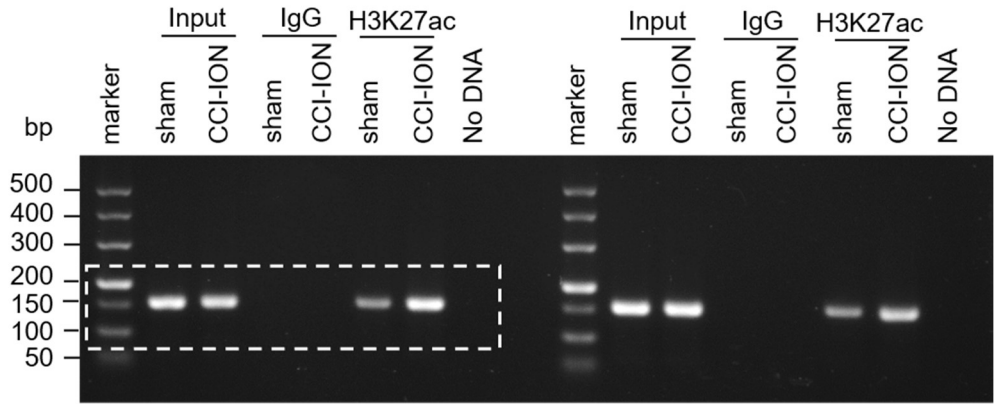


**Fig. S13: ChIP analysis indicating the binding of H3K27ac in the *Alkbh5* promoter in rat TGs following CCI-ION operation or sham surgery.** Shown is the full unedited gel for Fig. 4C.

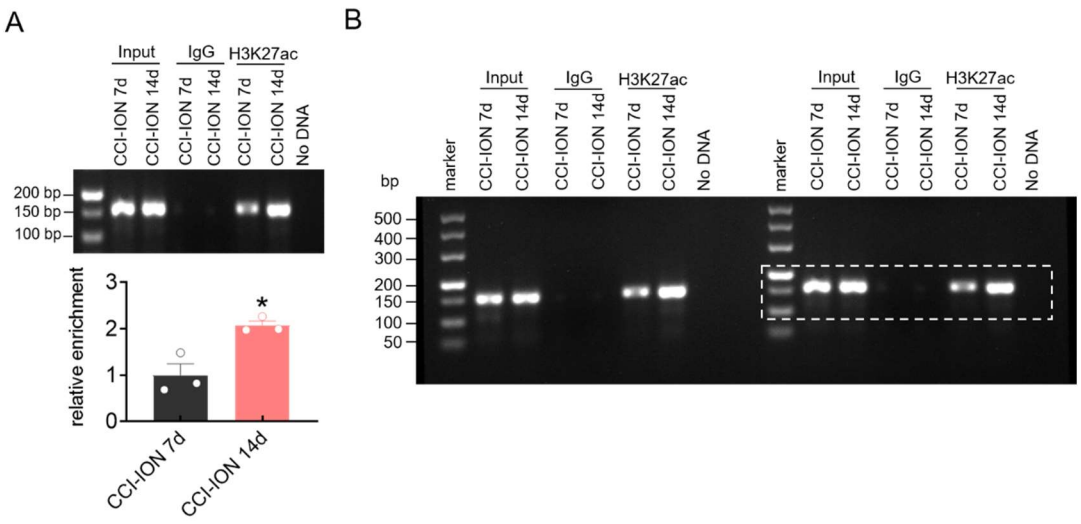


**Fig. S14:** (**A**) ChIP-qPCR analysis demonstrating that the binding activity of H3K27ac to the *Alkbh5* promoter was increased in the ipsilateral TG 14 days following CCI-ION compared with the CCI-ION group 7 days after surgery. Data were normalized to input and are expressed as the mean ± S.E.M. of three independent experiments. **p* < 0.05 *vs.* CCI-ION 7d (unpaired *t* test). *n* = 9 rats per group. (**B**) Shown is the full unedited gel for panel *A*.

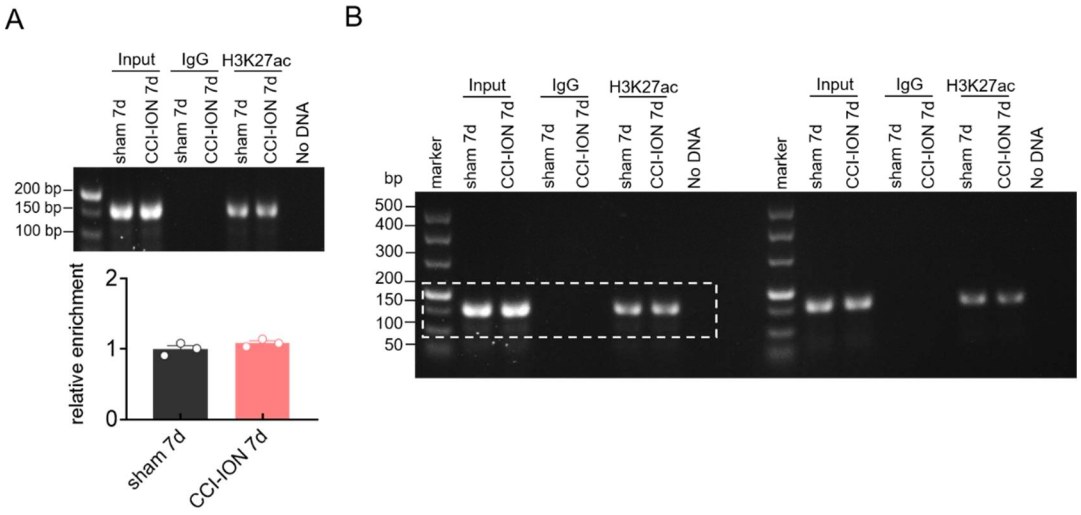


**Fig. S15:** (**A**) ChIP-qPCR analysis indicating the binding activity of H3K27ac to the *Alkbh5* gene promoter in the ipsilateral TG 7 days following CCI-ION operation or sham surgery. Data were normalized to input and are expressed as the mean ± S.E.M. of three independent experiments. *n* = 9 rats per group. (**B**) Shown is the full unedited gel for panel *A*.

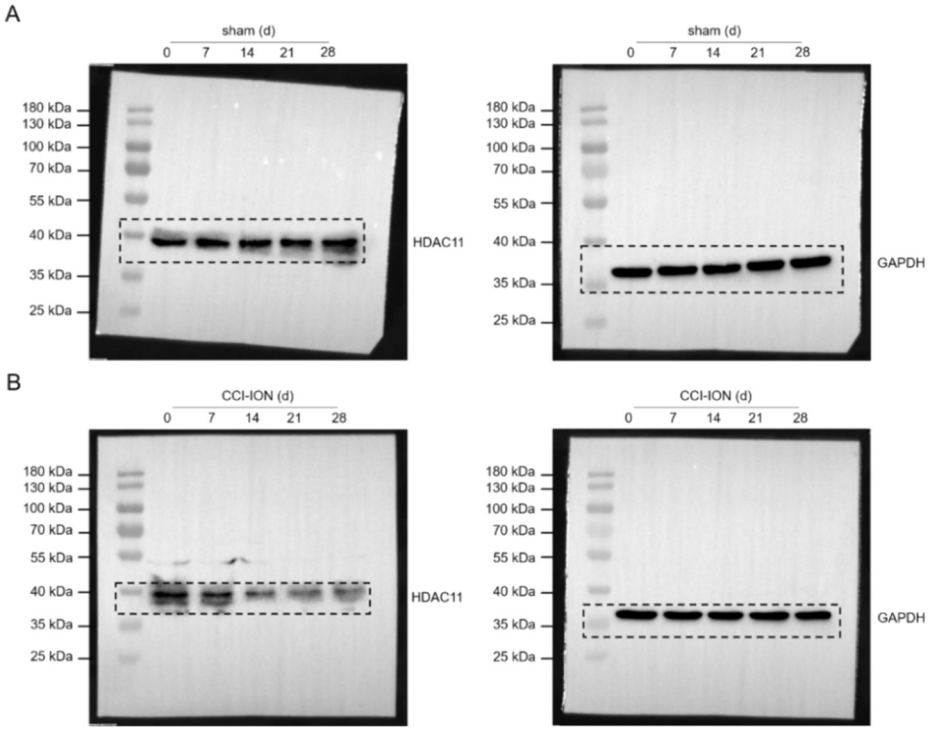


**Fig. S16: Protein expression of HDAC11 in rat TGs after sham surgery (*A*) or CCI-ION-operation (*B*).** Immunoblot images of the selected portion are displayed in Fig. 4E.

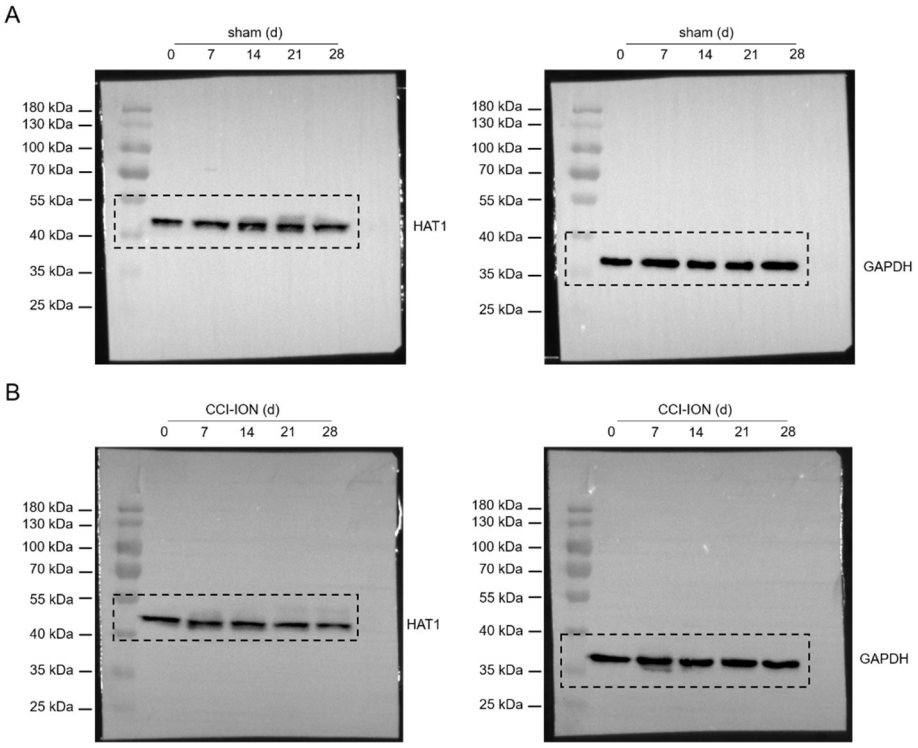


**Fig. S17: Immunoblot analysis of HAT1 in rat TGs after sham surgery (*A*) or CCI-ION-operation (*B*).** Western blot images of the selected portion are displayed in Fig. 4F.

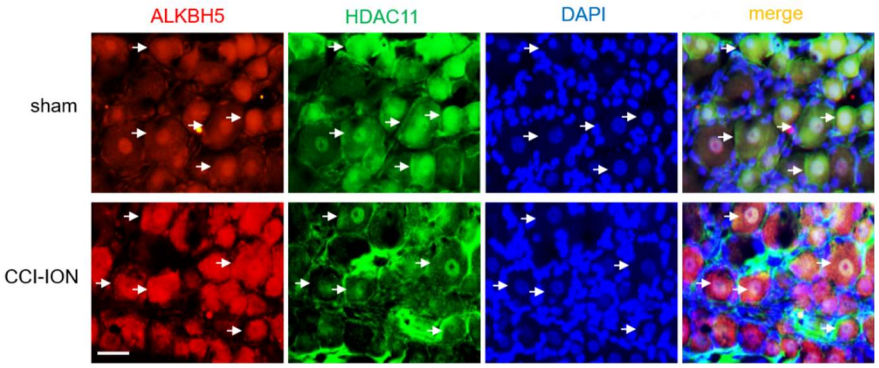


**Fig. S18: Double staining indicating the colocalization of ALKBH5 (*red*) with HDAC11 (*green*) and DAPI (*blue*) in rat TGs following CCI-ION operation or sham surgery.** Arrows show colocalization. Scale bar, 25 μm.

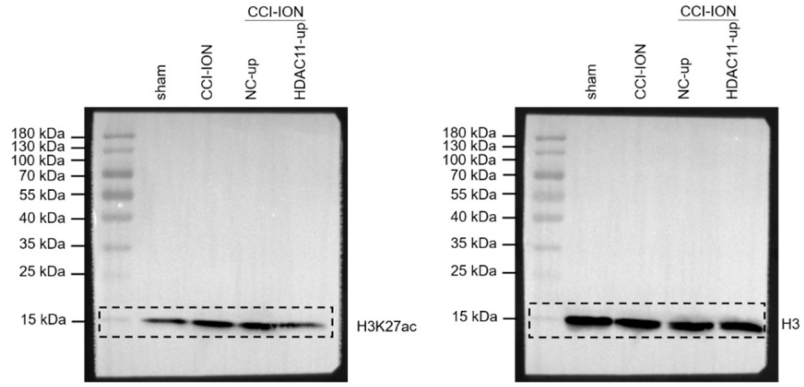


**Fig. S19: Administration of HDAC11-up prevented the increased expression of H3K27ac in the injured TG 14 days after CCI-ION.** Immunoblot images of the selected portion are displayed in Fig. 4G.

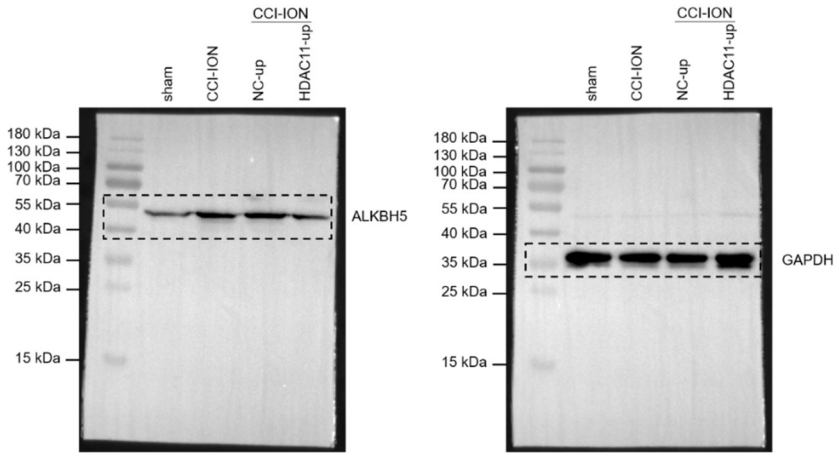


**Fig. S20: Administration of HDAC11-up prevented the increased expression of ALKBH5 in the injured TG 14 days after CCI-ION.** Immunoblot images of the selected portion are displayed in Fig. 4H.

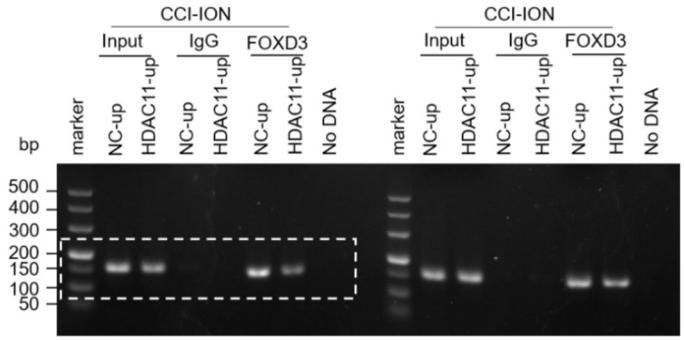


**Fig. S21: ChIP analysis indicating that administration of HDAC11-up decreased the binding activity of FOXD3 in the *Alkbh5* gene promoter in the injured TG 14 days post-CCI-ION.** Shown is the full unedited gel for Fig. 4I.

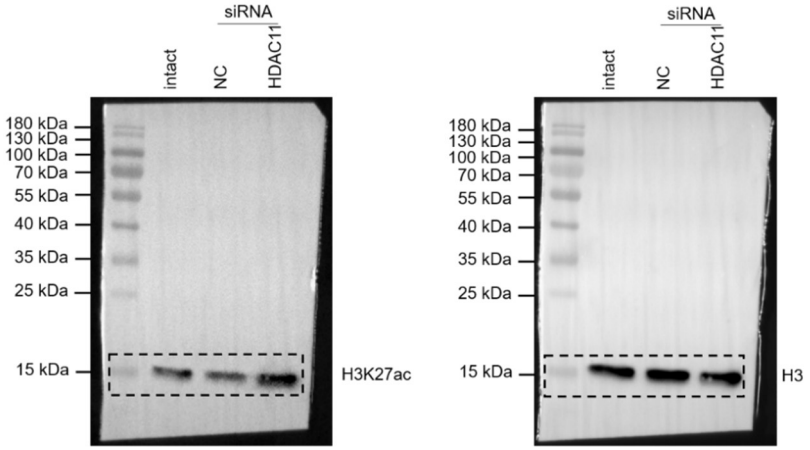


**Fig. S22: Administration of HDAC11-siRNA induced the increased expression of H3K27ac in the intact TG.** Immunoblot images of the selected portion are displayed in Fig. 4K.

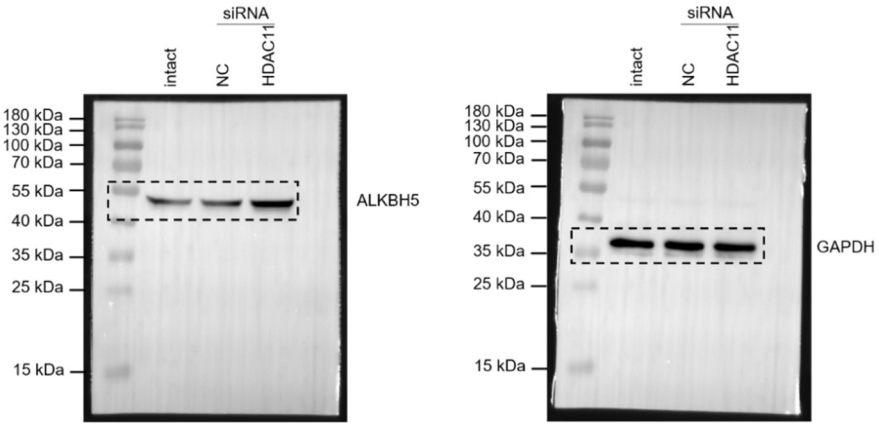


**Fig. S23: Administration of HDAC11-siRNA induced the increased expression of ALKBH5 in the intact TG.** Immunoblot images of the selected portion are displayed in Fig. 4L.

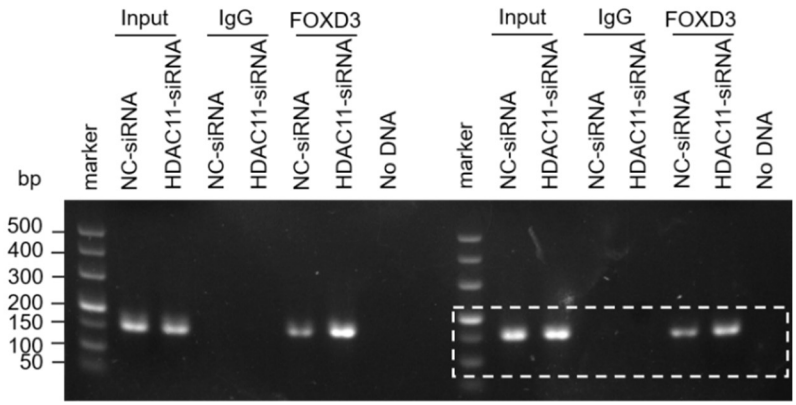


**Fig. S24: ChIP analysis indicating that administration of HDAC11-siRNA enhanced the binding activity of FOXD3 in the *Alkbh5* gene promoter in rat TGs.** Shown is the full unedited gel for Fig. 4M.

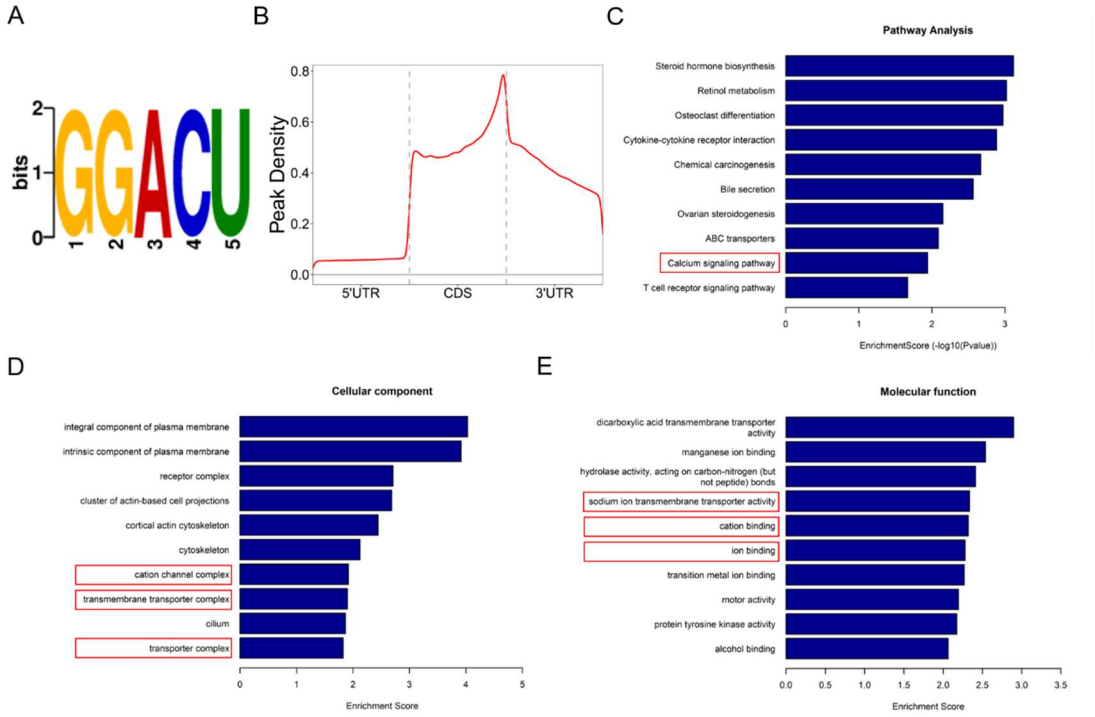


**Fig. S25:** (**A**) Sequence motif identified consensus motif within m6A peaks by MeRIP-seq. (**B**) Metagene profile demonstrating the distribution of m6A peaks across mRNA transcripts in rat TGs. (**C**) KEGG enrichment analysis showing the most enriched pathways correlated with ALKBH5-mediated m6A modification. (**D**) The cellular component of the identified genes was classified by GO analysis. (**E**) The molecular function of the identified genes was classified by GO analysis.

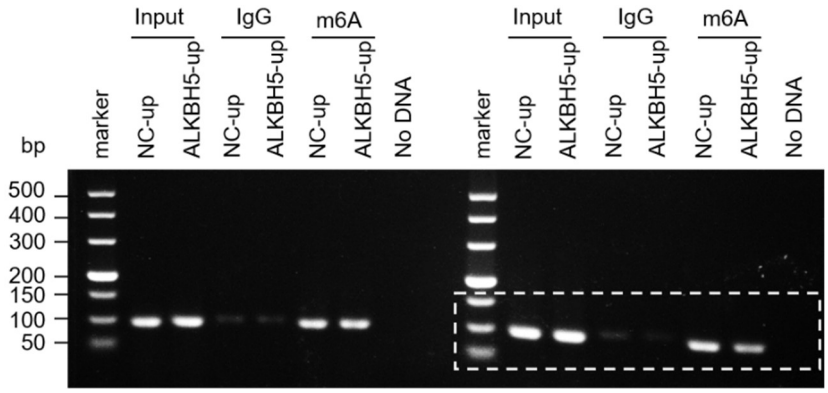


**Fig. S26: Intra-TG injection of ALKBH5-up decreased the m6A level in rat TGs.** Shown is the full unedited gel for Fig. 5D.

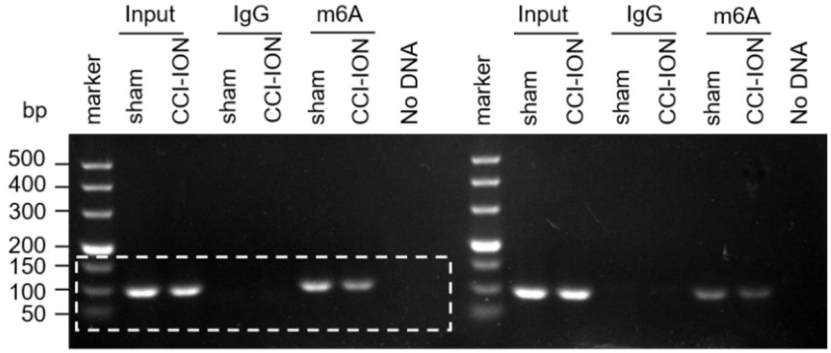


**Fig. S27: MeRIP-qPCR analysis showing the m6A level in rat TGs after CCI-ION or sham-operation.** Shown is the full unedited gel for Fig. 5E.

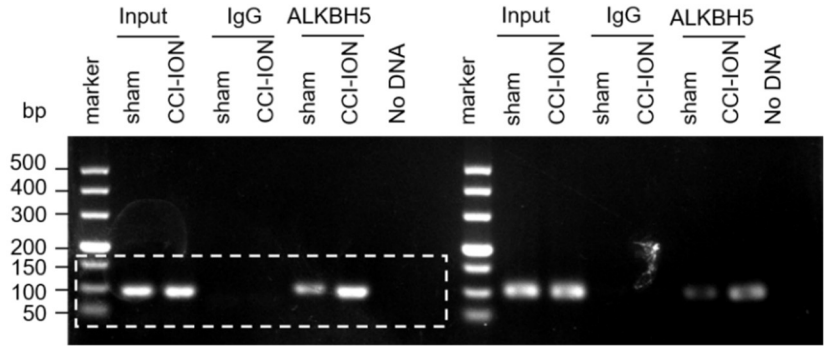


**Fig. S28: MeRIP-qPCR analysis showing the binding activity of ALKBH5 to *Htr3a* mRNA in rat TGs after CCI-ION or sham-operation.** Shown is the full unedited gel for Fig. 5F.

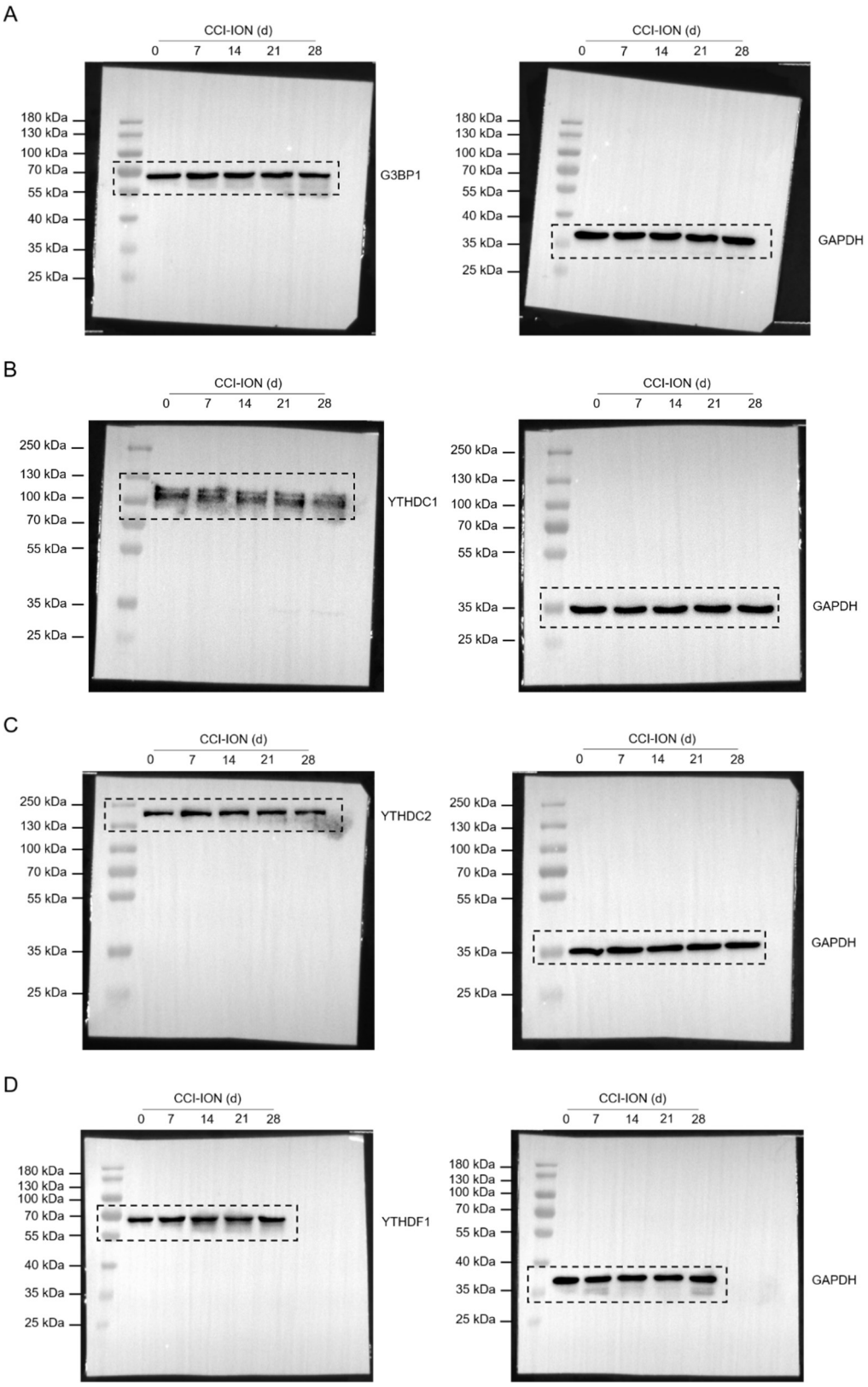
A
CCI-ION (d)
0 7 14 21 28
180 kDa
130 kDa
100 kDa
70 kDa
55 kDa
40 kDa
35 kDa
25 kDa
G3BP1
GAPDH
B
250 kDa
130 kDa
100 kDa
70 kDa
55 kDa
35 kDa
25 kDa
YTHDC1
GAPDH
C
YTHDC2
GAPDH
D
YTHDF1
GAPDH

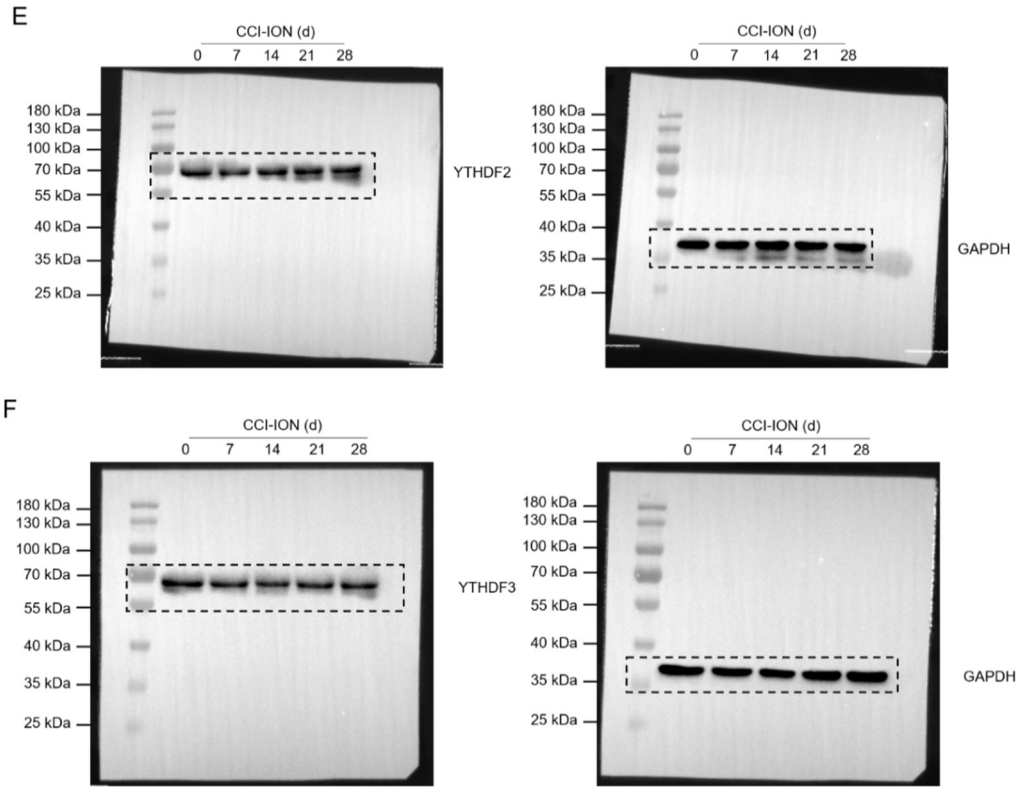


**Fig. S29: Protein expression of G3BP1 (*A*), YTHDC1 (*B*), YTHDC2 (*C*), YTHDF1 (*D*), YTHDF2 (*E*) and YTHDF3 (*F*) in rat TGs after CCI-ION.** Western blot images of the selected portion are displayed in Fig. 5H.

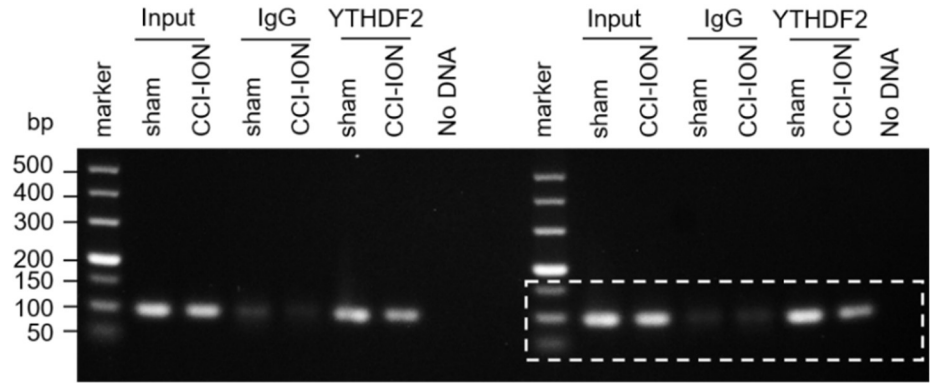


**Fig. S30: MeRIP-qPCR analysis indicating the binding of YTHDF2 to *Htr3a* mRNA in rat TGs after CCI-ION or sham-operation.** Shown is the full unedited gel for Fig. 5J.

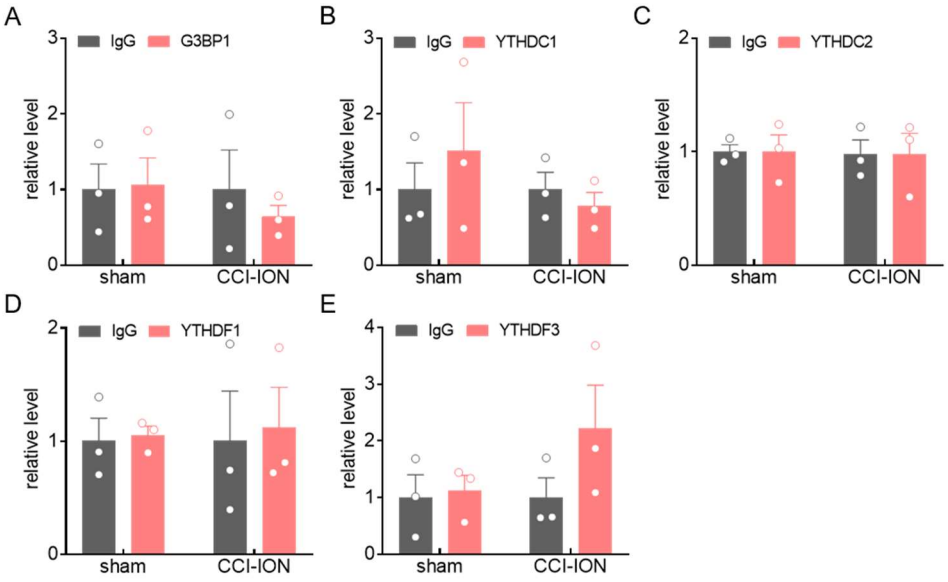


**Fig. S31: MeRIP-qPCR analysis shows the binding activity of G3BP1 (*A*), YTHDC1 (*B*), YTHDC2 (*C*), YTHDF1 (*D*) and YTHDF3 (*E*) in the *Htr3a* mRNAs in rat TGs following CCI-ION operation or sham surgery.** Data are representative of at least three experiments.

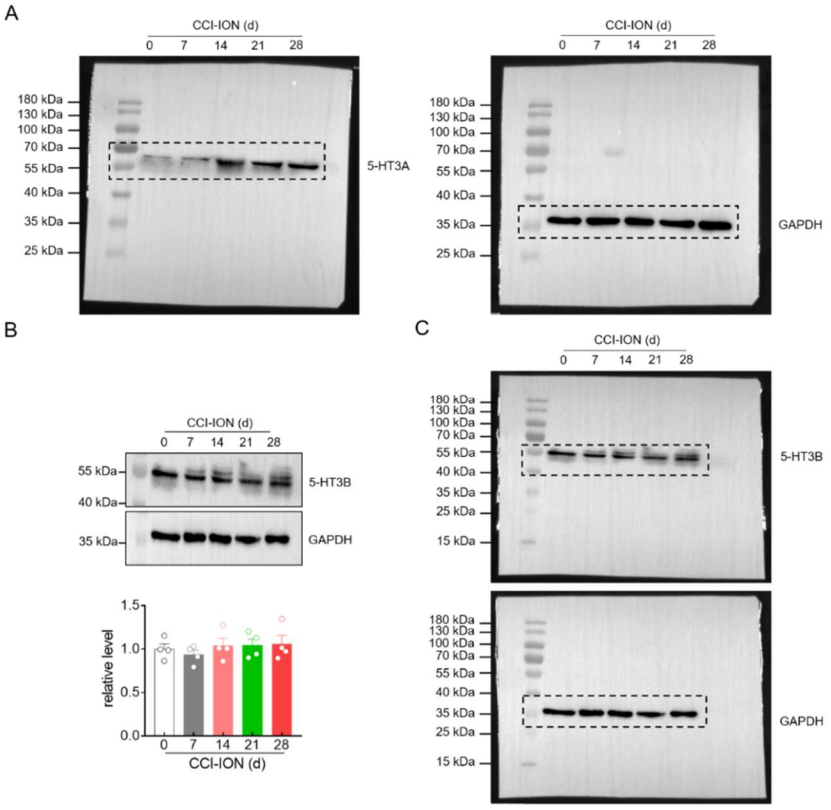


**Fig. S32: Immunoblot analysis of 5-HT3A and 5-HT3B in rat TGs following CCI-ION.** (**A**) Western blot images of the selected portion displayed in Fig. 6A. (**B**) CCI-ION did not change the protein abundance of 5-HT3B in the ipsilateral TG after surgery. (**C**) Immunoblot images of the selected portion are displayed in Panel *B*.

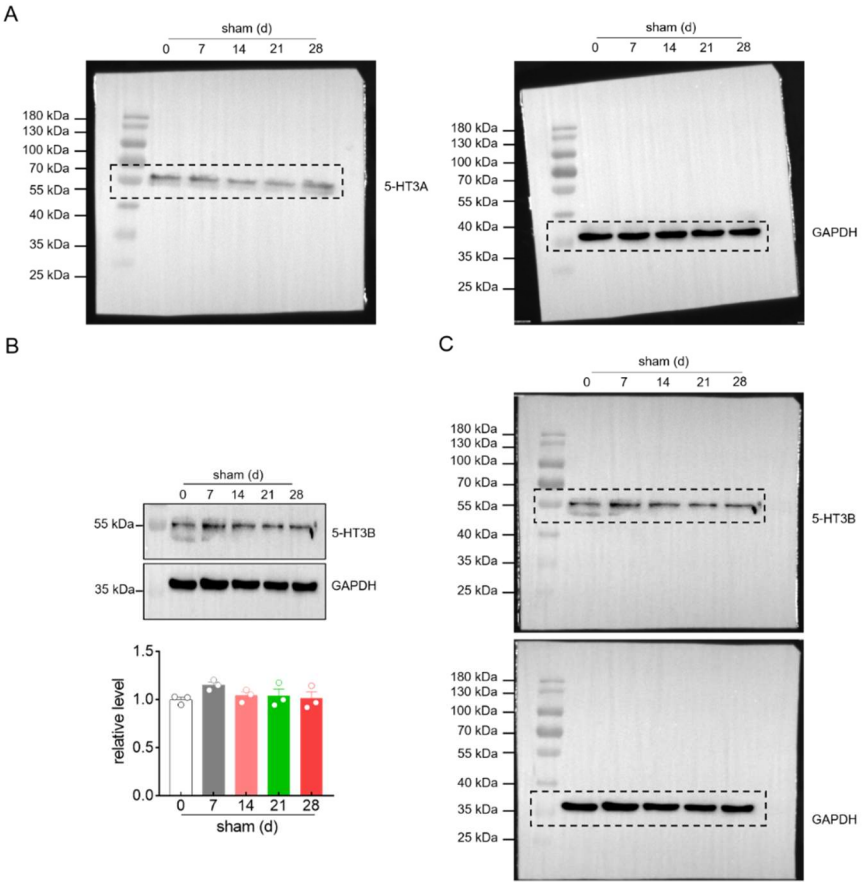


**Fig. S33: Protein expression of 5-HT3A and 5-HT3B in rat TGs following sham operation.** (**A**) Western blot images of the selected portion displayed in Fig. 6A. (**B**) The protein abundance of 5-HT3B remained unchanged in the ipsilateral TG following sham surgery. (**C**) Immunoblot images of the selected portion are displayed in Panel *B*.

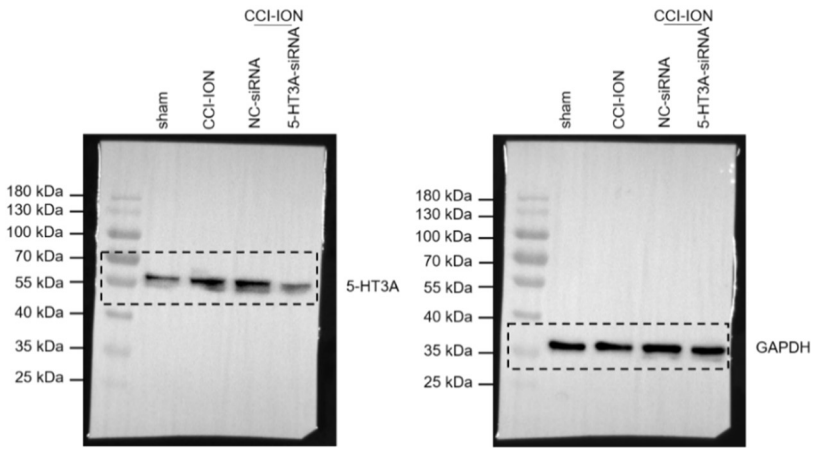


**Fig. S34: Administration of 5-HT3A-siRNA suppressed the increased 5-HT3A expression in the injured TG 14 days following CCI-ION.** Immunoblot images of the selected portion are displayed in Fig. 6F.

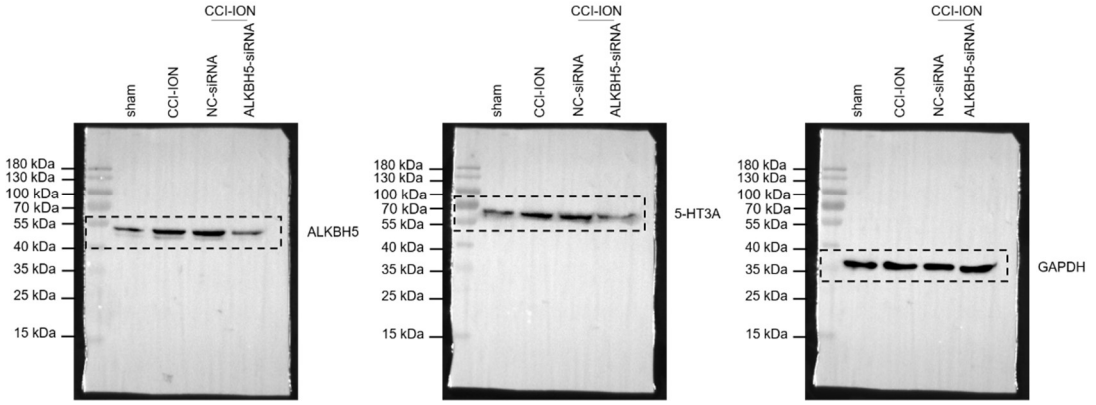


**Fig. S35: Administration of ALKBH5-siRNA suppressed the increased protein expression of ALKBH5 and 5-HT3A in the injured TG 14 days following CCI-ION.** Western blot images of the selected portion are displayed in Fig. 7A.

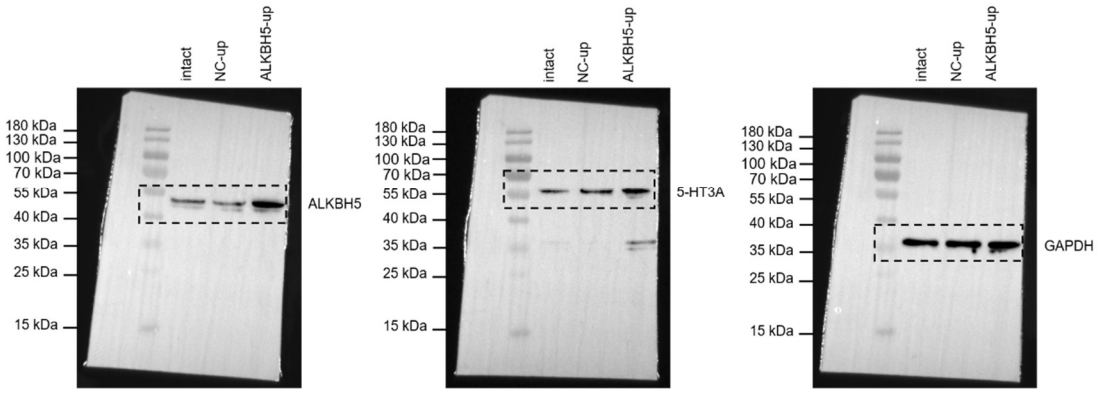


**Fig. S36: Administration of ALKBH5-up increased both the expression of ALKBH5 and 5-HT3A in the TGs.** Immunoblot images of the selected portion are displayed in Fig. 7C.

**SI Tables S1 to S2**

**Table S1: siRNAs used in the current study.**

| Name | Sense | Antisense |
|---|---|---|
| ALKBH5-siRNA | GGAUCCUGGAAAUGGACAATT | UUGUCCAUUUCCAGGAUCCTT |
| HDAC11-siRNA | GCAGACAUCACACUGGCUATT | UAGCCAGUGUGAUGUCUGCTT |
| 5-HT3A-siRNA | GCUCUGGUCCAUUUGGCAUTT | AUGCCAAAUGGACCAGAGCTT |
| NC-siRNA | GGCUCUAGAAAAGCCUAUGCTT | GCAUAGGCUUUUCUAGAGCCTT |

**Table S2: Sequences of nucleotides used in the current study.**

| Name | Forward | Reverse |
|---|---|---|
| GAPDH | GTGCTGAGTATGTCGTGGAGT | CAGTCTTCTGAGTGGCAGTGAT |
| METTL3 | CAGGGTCTGGATTGCGATGT | ATCCAGTTGGGCTGCACATT |
| METTL14 | GCTCTGGGGAAGGATTGGAC | TCGCTTCACGGTTCCTTTGA |
| WTAP | CGCAGGGAGAACATCCTTGT | CTCAGTTGGGCTACACTCGG |
| ALKBH5 | CCACATTGCCACCCAGCTAT | GGACTCATAGGACTTGCGCC |
| FTO | GGAGCGGGAAGCTAAGAAACT | GACCTCTTTGTGCAGCTCCT |
| G3BP1 | CATGTGGTCAAAGTGCCAGC | CCTTCGGGGTTCCACATCTC |
| YTHDF1 | TGCTGTTTTTGGGCAACCTG | GGGAGCTTGGTGGGTAAGTG |
| YTHDF2 | CAACAGACACAGCCATTGCC | TAGATCCAGAACCCGCCTGA |
| YTHDF3 | GGAGCGGGAAGCTAAGAAACT | GACCTCTTTGTGCAGCTCCT |
| YTHDC1 | ACCATTGGTGCAAAGCCAAC | TTGTTCTGGTTGAAGCCGGT |
| YTHDC2 | CCGATACGGTGACCAGAGAG | GCATGAGCTGTTTCTGATCCAT |
| FOXD3 | GACGGGCTGGAGGAGAAAGAC | GTGCCAGGGCTTGAGGTTGA |
| P300 | CCTAAATGCTTGCGGACTGC | GCCCAGATATGCCCTGTTGT |
| CBP | ACTGAAAATCCAGACATTTGGGC | ATCAATCTGCCCTTCCATGCT |
| KAT5 | GAAGACCTTGCCAATCCCG | GTTGAGCGGTGGTTGGGTT |
| KAT2a | GCTAACCTGAGCGAGTTGTG | CCTGCTTGGTGTCCGTGT |
| HDAC1 | TGCTAATGTTGGGAGGAGGTG | ATTGGAAGGGCTGATGTGAAG |
| HDAC2 | GCTGGGCTGCTTCAACCTAA | ACGTCCAACATCGAGCAACA |
| HDAC3 | CAGATCCGCCAGACCATC | GGCCTGCTGTAGTTCTCCTC |

| | | |
|---|---|---|
| HDAC4 | TGTCAGGCTTCCTTGTGG | TCTCCTCGGCATGGTGT |
| HDAC5 | TTCAACTCCGTAGCCATCA | GTTCCCATTGTCGTAGCG |
| HDAC6 | GGGCTGGTCTATGACGAAA | CCGAGCAGGTAGGATGAGA |
| HDAC7 | CTGTCAGACCCAAGTCCTCAAC | GCTCGGGATGCTTGCTGT |
| HDAC8 | AACTGGTCTGGAGGGTGG | ATTTCCGTCGCAATCGTA |
| HDAC9 | AGCCCAAGATACCAAGGATG | GCTGCTACTGACCGAGGATT |
| HDAC10 | GCTCCATCAAGAAGGGTCAG | CAGGATTCCATCTAAGAGGCAC |
| HDAC11 | TTACAACCGCCACATCTACCC | CTCCACCTTCTCCAGATACTCCTC |
| HAT1 | ATGGCGATACAGGCACAG | CAGGCATTTCCTCATCTTGG |
| HTR3A | GACCGCCTGTAGCCTTGACA | CTCCCACTCGCCCTGATTT |
| ATP1A4 | ACAAGACTGGCACCCTCACC | CCCTGTTGTTGTCCGCTTAGTT |
| ATP2B3 | AGTTCCATTGAGTTCCACCCC | CCACTGACATCCCCATAGGCT |
| CACNA1G | GGACTGATGACCCCCAACTG | GACCAGGAATCTCGCTCTCG |
| HTR5B | GCCGTGGTGCTCTTCGTCTA | TGCTTCCTTTGCCTGCGTG |
| PDE1B | GATCTTCGTGGAGCGGATGT | GAAGCGGCTGATGAGGCTAT |
| PKD1L3 | GAATCAGTGTCGTTTTGGGTGT | CTTTTGGGGAGAGTTCTGTAGG |
| PTK2B | CACAGTCCATCCAGCCTACAG | ACCACCACCACATACTCCTCA |
| SCN5A | TGCATTCACCTTCCTTCGGG | GGTGCGTAAGGCTGAGACAT |
| TRPC6 | CAGGATCAATGCCTACAAAG | CAGGAGACCCACAACAAAAT |
| ChIP | GTGGCGTGAAGGCAAATTGT | CCACGAGACTCCACGTACTC |
| RIP | GGCTTCTTCTTCAGCTCACTTGT | CATAGCATTTTATTATTCCCTCCC |
| Luc-pGL3-F1 | GGGGTACCGGTTCCACGAAAGTCCAG | CTAGCTAGCTTATCCCTGTCCCTCCTG |
| Luc-pGL3-F2 | | CTAGCTAGCGGCTGGGCGTTGTTAT |
| Luc-pGL3-F3 | | CTAGCTAGCGGCTACTGCGTCCATCAC |
| Luc-pGL3-F4 | | CTAGCTAGCCTTAGCGGGCTTCTCG |
| Luc-pGL3-F5 | | CTAGCTAGCCCCGCCAACTCAACTCT |